Cellular mechanisms for integral feedback in visually guided behavior

Bettina Schnell[a,b,1], Peter T. Weir[a], Eatai Roth[a], Adrienne L. Fairhall[b], and Michael H. Dickinson[a]

Departments of [a]Biology and [b]Physiology and Biophysics, University of Washington, Seattle, WA 98195

Edited by Terrence J. Sejnowski, Salk Institute for Biological Studies, La Jolla, CA, and approved March 7, 2014 (received for review January 14, 2014)

Sensory feedback is a ubiquitous feature of guidance systems in both animals and engineered vehicles. For example, a common strategy for moving along a straight path is to turn such that the measured rate of rotation is zero. This task can be accomplished by using a feedback signal that is proportional to the instantaneous value of the measured sensory signal. In such a system, the addition of an integral term depending on past values of the sensory input is needed to eliminate steady-state error [proportional-integral (PI) control]. However, the means by which nervous systems implement such a computation are poorly understood. Here, we show that the optomotor responses of flying *Drosophila* follow a time course consistent with temporal integration of horizontal motion input. To investigate the cellular basis of this effect, we performed whole-cell patch-clamp recordings from the set of identified visual interneurons [horizontal system (HS) cells] thought to control this reflex during tethered flight. At high stimulus speeds, HS cells exhibit steady-state responses during flight that are absent during quiescence, a state-dependent difference in physiology that is explained by changes in their presynaptic inputs. However, even during flight, the membrane potential of the large-field interneurons exhibits no evidence for integration that could explain the behavioral responses. However, using a genetically encoded indicator, we found that calcium accumulates in the terminals of the interneurons along a time course consistent with the behavior and propose that this accumulation provides a mechanism for temporal integration of sensory feedback consistent with PI control.

feedback control | insect vision | lobula plate tangential cells | fruit fly

A common strategy for maintaining a straight course is to steer such that the apparent rotation of the visual scene on the retina is continuously minimized. This stabilization can be achieved with a simple control system in which the rate of turning is proportional to the instantaneous value of the measured error signal. In the case of a yaw control system, the relevant error signal is the rotational optic flow on the retina. However, control systems that rely solely on a proportional response cannot achieve zero steady-state error (1). In the case of a yaw regulator, this small uncorrected error would result in the animal rotating in one direction. This steady-state bias could be corrected either by orienting to an absolute positional cue (landmark) or by incorporating a feedback component commensurate to the temporal integral of the error signal. In engineering applications, integral feedback is almost always included in the control signal to the actuator system, creating a proportional-integral (PI) controller (1). The integral term speeds convergence to zero error and avoids small steady-state offsets that plague systems relying on proportional feedback alone. Here, we provide evidence for temporal integration of visual feedback during flight in the fruit fly, *Drosophila*, and exploit the genetic tools available to elucidate the underlying cellular mechanisms.

In the optomotor response, flies compensate for deviations from a straight flight path by turning in the direction of large-field visual motion (2). The horizontal system (HS) cells, three bilateral pairs of lobula plate tangential cells (LPTCs), are thought to provide the primary source of visual feedback for this behavior in response to horizontal motion (3–6). HS cells respond to horizontal motion in a directionally selective manner by depolarizing in response to preferred direction (PD) and hyperpolarizing in response to null direction (ND) motion (7, 8). They receive directional-selective input from a subset of columnar T4 and T5 cells (9, 10), of which four variants arborize in different layers in the lobula plate, creating a map of motion directionality (11).

A well-established model for elementary motion detection in insects, the Hassenstein–Reichardt detector, predicts many response properties of LPTCs, including a dependence on temporal frequency (12, 13). However, the responses of HS cells are not entirely consistent with those of the behavior they are thought to drive. For example, they exhibit a temporal frequency optimum near 1 Hz in quiescent flies (7), whereas the behavioral response optimum reported in flying flies is significantly higher (3–10 Hz) (14–17). It has been proposed that this discrepancy is due to differences in the response properties of LPTCs during walking and flight compared with quiescence (18–20), although the actual responses of HS cells during flight have not been reported. Here, we show that HS cells exhibit increased steady-state responses during flight compared with quiescence. This increase, however, is not sufficient to explain the time course of the optomotor behavior in response to constant visual motion. Instead, we propose that there is a temporal integration step in the optomotor pathway that is performed by calcium accumulation in the terminals of the HS cells.

Significance

Visually driven behaviors of *Drosophila* have become a model system to study how neural circuits process sensory information. Here, we show that one of the computations performed by this system is temporal integration of visual motion. We provide evidence of how this computation might be performed by measuring the activity of identified visual interneurons during tethered flight that are thought to control the described behavior: Presynaptic calcium accumulation in these neurons mimics a leaky temporal integration of the visual motion signal as does the behavior. In the future, the genetic tools available in *Drosophila* will enable studying the precise mechanism of temporal integration in this model system, which could provide insights into general mechanisms of neuronal information processing.

Author contributions: B.S., P.T.W., A.L.F., and M.H.D. designed research; B.S., P.T.W., and E.R. performed research; B.S., P.T.W., and E.R. analyzed data; and B.S., P.T.W., A.L.F., and M.H.D. wrote the paper.

The authors declare no conflict of interest.

This article is a PNAS Direct Submission.

Freely available online through the PNAS open access option.

[1]To whom correspondence should be addressed. E-mail: bschnell@uw.edu.

This article contains supporting information online at www.pnas.org/lookup/suppl/doi:10.1073/pnas.1400698111/-/DCSupplemental.

Results

We performed whole-cell patch-clamp recordings from HS cells during tethered flight (Fig. 1 *A* and *B*). At the start of flight, we recorded an increase in membrane potential from −42.2 mV (± 0.07 mV SEM) to −40.1 mV (±0.12 mV SEM), an effect that was similar in magnitude to what has been observed in vertical system (VS) cells (20, 21). To directly compare behavioral and neuronal responses, we first presented a square-wave grating moving horizontally at different velocities. In between stimulus presentations, the flies performed closed-loop stripe fixation, which typically induces longer flight bouts. An example trace of an HS cell recording with the simultaneously measured behavioral output during flight is shown in Fig. 1*C*. For comparison, a response of the same HS cell during quiescence (i.e., when the animal was not flying) is shown below. Both the membrane potential of HS cells in the right hemisphere and the difference in wing stroke amplitude of the left and right wing (L-R) increase in response to rightward motion. However, flies occasionally perform fast turns in the opposite direction of stimulus motion, which probably correspond to body saccades in free flight (22, 23). Remarkably, these internally generated turns coincide with brief changes in the membrane potential of HS cells (indicated by the arrowheads in Fig. 1*C*). This effect might serve to counteract the response of HS cells to the visual stimulus that would normally be elicited by an active flight maneuver. Whereas this phenomenon was a consistent feature of HS cell physiology during flight, it was not the focus of this study and we have ignored these events in our subsequent analysis.

We found evidence for temporal integration in the optomotor system when comparing the time courses of HS cell activity and steering responses elicited by a square wave grating moving horizontally at different velocities. At low temporal frequencies (i.e., low stimulus velocities), both the behavioral turning responses (L-R) and the change in membrane potential of HS cells remain elevated throughout stimulus presentation (Fig. 1*D, Left*). At high temporal frequencies, however, HS cells exhibit a transient depolarization followed by adaptation to a low steady-state level, whereas the behavioral responses remain constant throughout stimulus motion (Fig. 1*D, Right*). During quiescence, HS cells exhibit even stronger adaptation (Fig. 1*D*, black traces). Based on these data, we constructed steady-state temporal frequency tuning curves by subtracting the steady-state responses (measured as the mean response during the interval of 1–2 s of stimulus presentation) to preferred and null direction motion (PD and ND, respectively; Fig. 1*E*). Whereas the HS cell tuning curve shows a distinct maximum, the behavioral tuning curve is quite broad. Differences in the shapes of these tuning curves have been attributed to the effects of neuromodulation on the motion vision pathway during flight (19). However, the temporal frequency tuning curve of HS cells measured during flight does not resemble the behavioral tuning curve. Instead, we propose that the broad plateau of the behavioral tuning curve is evidence for a leaky temporal integrator in the optomotor pathway. For long stimulus durations, the behavioral output asymptotes to approximately the same maximum value at all temporal frequencies and, thus, does not reflect the current value of the membrane potential of HS cells, but rather its short-term history.

To obtain direct estimates of the temporal filtering properties of both the behavior and the HS cell response, we determined their impulse responses by using an m sequence (24, 25). An m sequence is a pseudorandom binary sequence controlling, in this case, the instantaneous velocity of the pattern (Fig. 2*A, Top*). The pattern was a sine wave grating moving one pixel (2.25°) in

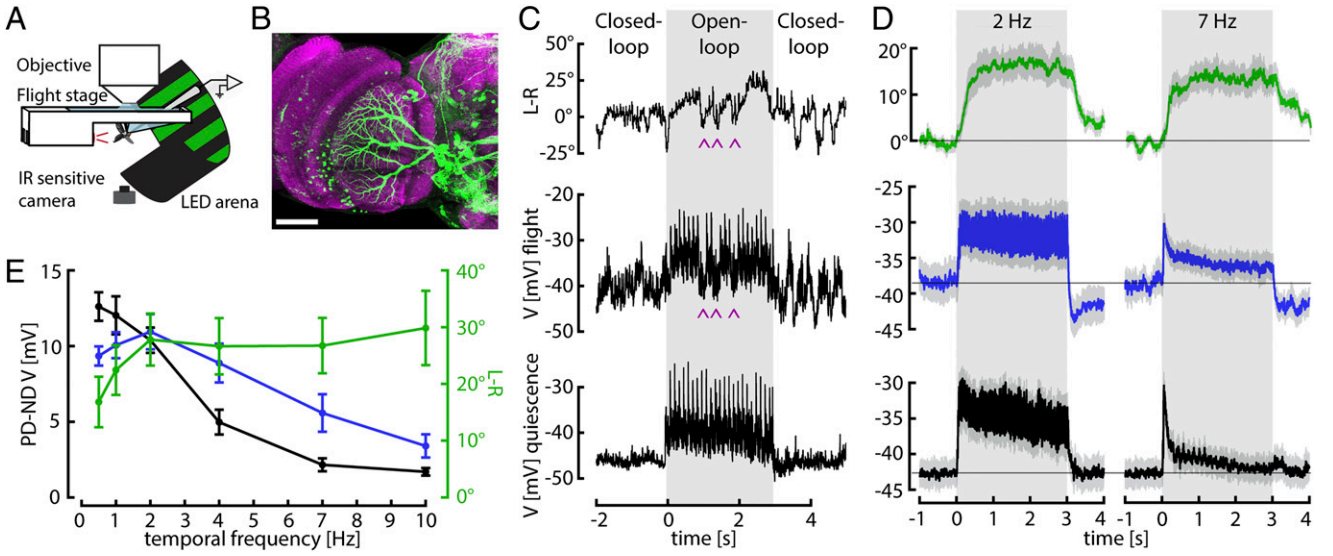

Fig. 1. Simultaneous neuronal and behavioral recordings. (*A*) Schematic of the setup for whole-cell patch-clamp recordings during flight. (*B*) Maximal intensity projection of the Gal4 line R27B03 crossed to UAS-eGFP showing the dendrites of three labeled HS cells of one lobula plate (approximately 30 μm in depth) in green. Neuropil staining shown in purple. (Scale bar: 50 μm.) (*C*) Example traces obtained from one fly. Periods of closed-loop stripe fixation are interspersed with 3 s of open-loop stimulus presentation (shaded gray areas), when a square wave pattern drifts horizontally in the cell's preferred direction (PD) (here at 0.5 Hz temporal frequency). The traces indicate the optomotor behavior measured as difference between wing stroke amplitudes (L-R), the membrane potential (V) of an HS cell recorded simultaneously, and the response of the same HS cell to a similar stimulus during quiescence. HS cells depolarize in response to PD motion and hyperpolarize in response to null direction (ND) motion (Fig. S1). The motor output shows a similar directional dependence. Rightward stimulus motion elicits increases in L-R, corresponding to a right turn. During the closed-loop portion of the flight trials, the cells responded robustly to the horizontal motion of the stripe. Flies occasionally perform fast turns in the opposite direction of stimulus motion. These internally generated turns coincide with brief changes in the membrane potential of HS cells (purple arrowheads). (*D*) Mean and SEM (gray envelopes) of behavioral (L-R, green) and neuronal responses during flight (blue) and quiescence (black) of 11 flies for temporal frequencies of 2 and 7 Hz. Light gray areas indicate time of stimulus motion. (*E*) Mean and SEM of steady-state HS cell responses during quiescence (black) and flight (blue) and of behavioral responses (green), calculated during the second second of open-loop stimulus presentation. ND responses (Fig. S1) were subtracted from PD responses.

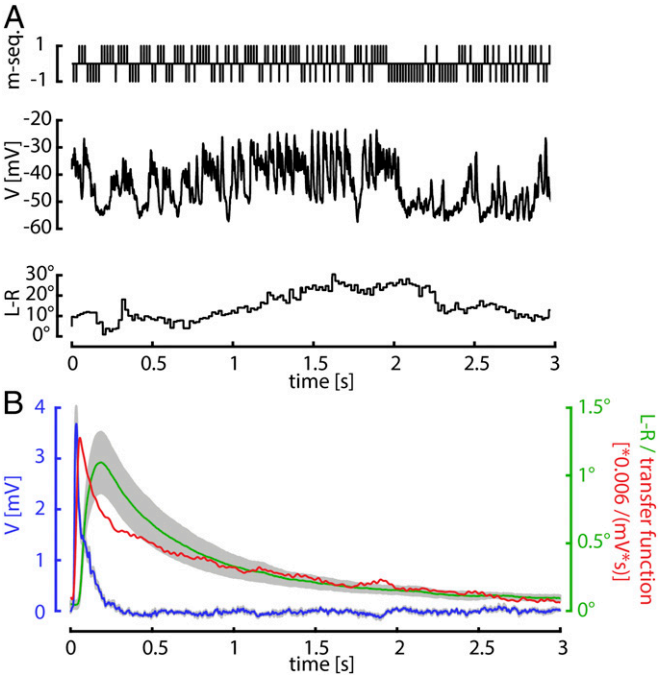

Fig. 2. HS cell and behavioral impulse responses. (*A*) Example trace of an m-sequence experiment. An m-sequence controls the instantaneous horizontal velocity of a large field sine grating. +1 (−1) indicates that the stimulus was moving in the PD (ND) of the cell. The change in membrane potential (V) of one HS cell and the turning response (L-R) elicited by this stimulus are shown below. (*B*) Mean neuronal (blue, $n = 5$) and behavioral (green, $n = 4$) impulse responses obtained from m-sequence data. SEM is indicated in gray. Behavioral data were obtained from intact flies by using a longer m-sequence than for neuronal data. The red line is the transfer function (TF) between the two responses.

PD for every 1 and one pixel (2.25°) in ND for every −1. For electrophysiological experiments, a 10th-order m sequence was presented at frequencies between 35 and 80 Hz. Convolving the stimulus with the HS cell responses during flight (Fig. 2*A, Middle*) and the simultaneously measured turning responses (L-R) (Fig. 2*A, Bottom*) gives an estimate for the impulse response of the cell and the behavior (Fig. 2*B* and Fig. S2). The impulse response of HS cells rises sharply and decays to zero in less than 400 ms (Fig. 2*B*, blue line). The decay of the neuronal response is well approximated by an exponential with a time constant of 65 ms (least square fit, $R = 0.936$). Because the behavioral response during physiological recording exhibited a longer time constant (Fig. S2), we obtained additional behavioral data from intact wild-type flies (without recording neuronal responses) by using a longer (15th order) m sequence. The behavioral impulse response is broader than that of the HS cells and decays with a much slower time course (Fig. 2*B*, green line). The decay of the behavioral response is well approximated by the sum of two exponentials with time constants of 0.52 s and 4.44 s (least square fit, $R = 0.996$). The transfer function with which the neuronal response would have to be convolved to produce the behavioral response (Fig. 2*B*, red line) accordingly has an initial peak and a very long tail and is thus suggestive of a leaky integrator between HS cells and motor output.

Because behavioral responses to the m-sequence stimulus are relatively small, we performed a further test for the presence of integration in the horizontal motion pathway. We presented flies with a grating moving horizontally at a temporal frequency of 7 Hz across a range of stimulus durations and measured behavioral responses of intact flies during the stimulus motion and the subsequent 3 s during which the stimulus was stationary (Fig. 3*A* and Fig. S3). Evidence for an integral term in the sensory-motor system was manifest by two features of the behavior: a rise in the peak motor response with longer stimulus durations (Fig. 3*E*, green trace) and a very slow decay of the turning response after the stimulus motion ceased. The persistence of the motor response following the offset of visual motion is particularly striking, given the brevity of steering maneuvers in freely flying flies (26).

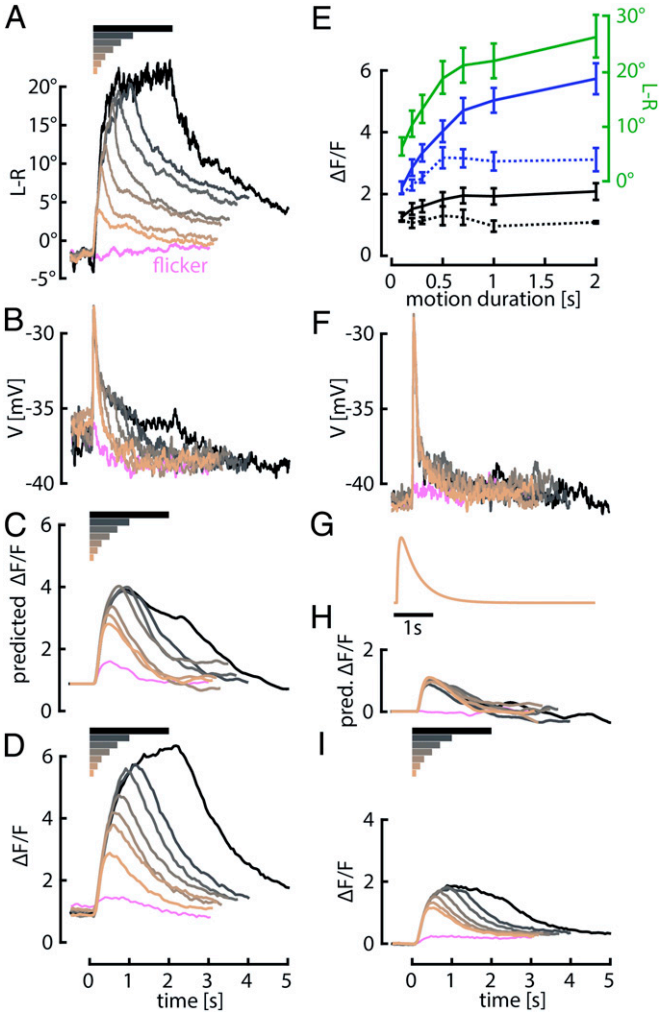

Fig. 3. Behavioral and HS cell responses to motion stimuli of variable duration. (*A*) Mean behavioral responses of 15 intact wild-type flies to a large-field pattern rotating in the PD for a variable length of time (from 0 to 2 s, indicated by the horizontal bars above) and then remaining stationary for 3 s. Before the stimulus, flies performed closed-loop stripe fixation. (*B*) Mean membrane potential (V) of HS cells during flight in eight flies in response to the same stimuli. (*C*) Prediction of the fluorescence signal based on reported time constants of GCaMP6f estimated by convolving baseline-subtracted neuronal responses in *B* with the kernel shown in *G*. Predictions were normalized to the peak response of the shortest duration trial. (*D*) Measured GCaMP6f fluorescence changes ($\Delta F/F$) in the terminals of HS cells of 21 flies during flight in response to similar stimuli as in *A* and *B*. (*E*) Mean and SEM of behavioral responses (green solid line) and peak predicted (dotted lines) and measured (solid lines) fluorescence changes during flight (blue) and quiescence (black) from *A*, *C*, *D*, *H*, and *I* plotted against stimulus duration. The baseline (mean during 0.5 s before open-loop stimulus) was subtracted from the measured GCaMP6f responses. (*F*, *H*, and *I*) Same as *B–D*, but during quiescence. (*G*) Kernel for predicting fluorescence changes purely based on GCaMP6f dynamics. Time constants for rise and decay ($\tau_{0.5}$) are 50 and 490 ms, respectively, and were chosen to match the prediction to the time course of the imaging data for the shortest duration stimulus (0.1 s) in *D*.

The membrane potential responses of the HS cells do not, however, resemble a temporal integration of the stimulus input (Fig. 3 *B* and *F*). During quiescence the responses are nearly identical for all stimulus durations, consisting of a brief transient at the onset of motion followed by a rapid decay (Fig. 3*F*). The membrane potential response more closely resembles a differentiation of the visual motion input than integration. During flight, the cells respond with a transient depolarization of the same peak magnitude, but followed by a small plateau response that lasts for the duration of the stimulus (Fig. 3*B*). The discrepancy with the behavior is somewhat puzzling given that HS cells are thought to be only a few synapses upstream of the motor neurons driving wing motion.

One possible explanation for this discrepancy is that the membrane potential of an HS cell does not provide an accurate measure of its synaptic output. Assuming that some HS cell connections are mediated by chemical synapses, the calcium levels in the terminals of the neurons could have different dynamics and provide a mechanism for temporal integration. To test this hypothesis, we expressed the genetically encoded calcium indicator GCaMP6f (27) in HS cells (Fig. S4) and performed a set of two-photon imaging experiments during flight with a protocol similar to that used during whole-cell recordings. In contrast to the membrane potential responses, the GCaMP6f signals from HS cell terminals are consistent with the behavioral results in that they increase with increasing stimulus duration and decay very slowly after the end of motion (Fig. 3*D*).

The fluorescence changes we measured in the HS cells are determined by the time history of free calcium within the cell and the dynamics of GCaMP6f binding. To estimate the influence of indicator binding dynamics on the signals, we constructed a GCaMP6f response kernel based on our data (Fig. 3*G*). The rise and decay time constants were chosen such that a convolution of the kernel with the membrane potential response to the shortest duration stimulus best matched the measured GCaMP6f response during flight. The time constants obtained in this manner were quite similar to reported on and off rates of GCaMP6f (27). Based on this consistency, we predicted the fluorescence responses to different stimulus durations by convolving the GCaMP6f kernel with the electrophysiological responses to those stimuli. The resulting predictions should represent a conservative estimate for how the temporal dynamics of the indicator filter the actual calcium changes in HS cells. In the case of a quiescent fly, our model predicts that the fluorescence changes induced by visual motion should change little with increasing stimulus length (Fig. 3*H*). The actual measured GCaMP6f responses, however, grow measurably with stimulus duration (Fig. 3*I*). This discrepancy suggests that nonlinear processes within the HS cells strongly magnify small differences in membrane potential and allow calcium to accumulate in the terminals according to a time scale that cannot be explained by the binding rates of the indicator.

The predicted and measured GCaMP6f signals from flying flies differ from the quiescent case in several ways. First, the magnitude of the measured GCaMP6f signals in HS cells is substantially larger during flight, to a degree that is not proportional to the differences in membrane potential. Second, based on convolving our estimated indicator kernel with the measured membrane potential responses, we predict that the GCaMP6f signal should rise with increasing stimulus length. This growth of the predicted response curves with stimulus duration is due to the low-pass filtering characteristics of the indicator acting on the small but consistent plateaus of the membrane potential during flight (Fig. 3*B*) that are not present during quiescence (Fig. 3*F*). However, the predicted responses during flight severely underestimate the magnitude and long decay of the measured GCaMP6f signals, as was the case during quiescence (except for the shortest duration trial used to fit the kernel parameters). The failure of the model provides evidence of calcium accumulation within the terminals of the HS cells. Furthermore, the measured GCaMP6f signals during flight (Fig. 3*D*) bear a strong resemblance to the behavioral output (Fig. 3*A*).

To better illustrate the degree of integration, we plotted peak responses as a function of stimulus duration for the predicted and measured GCaMP6f data (Fig. 3*E*, blue and black traces). GCaMP6f signals in the terminals of the HS cells rise with stimulus duration until saturation in a manner that represents an integration of the visual motion input and closely matches the optomotor behavior. The integration timescale imparted by the indicator dynamics falls short of predicting the strong increase of signal with increasing stimulus duration. It is also informative to compare the results of quiescent and flying flies. Not only are the GCaMP6f signals smaller during quiescence, they do not exhibit the degree of integration during flight as indicated by the shallower slope and earlier saturation.

The prolonged response plateaus in HS cells recorded during flight, although small as measured in the cell body, might be important for generating the calcium accumulation in the terminals. These plateaus are absent during quiescence, which correlates with the reduced accumulation of calcium. The appearance of these plateaus during flight might result from modulation of intrinsic HS cell properties or alternatively could reflect changes in their synaptic drive. To address this question, we expressed GCaMP6f in T4 and T5 cells that provide directional motion information to LPTCs (9, 10) (Fig. 4*A*). We measured fluorescence changes in the HS cell layer of the lobula plate in response to a similar set of horizontal motion stimuli of different durations during quiescence and flight. In contrast to

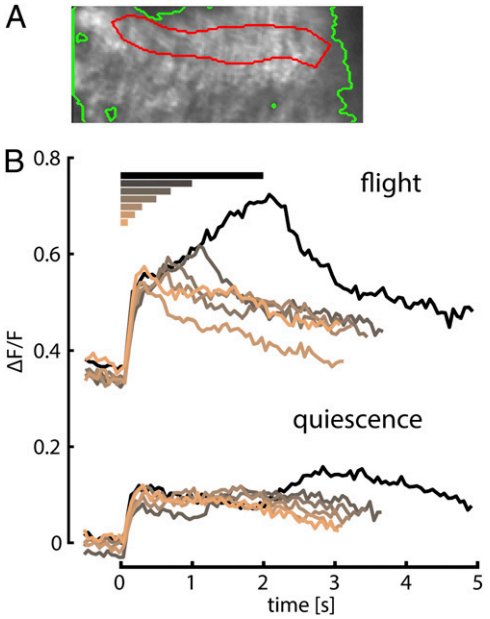

Fig. 4. T4 and T5 cell responses to stimuli of varying durations similar to Fig. 3. (*A*) Mean image of T4 and T5 cell terminals in the lobula plate obtained during recording from one fly with the region of interest circled in red and the background in green. In this image, medial would be on the top, lateral on the bottom, dorsal to the right, and ventral to the left. The region of interest was chosen to match the layer of HS cell dendrites, which is the deepest layer (in this view most medial) next to the lobula, where T5 cells have their dendrites. (*B*) Fluorescence changes in the HS cell layer during quiescence (lower traces) and flight (upper traces) of 10 flies. The grating was held stationary in between trials and started moving at time 0 for the time indicated by the colored bars on top of the graph.

the previous experiments, we held the square-wave grating stationary during the segments between motion trials, because in initial experiments, T4 and T5 cells exhibited a strong response to just the presentation of the stationary grating, which made it difficult to discriminate responses to motion of different durations if the pattern started moving immediately after appearing. During quiescence, responses to all different durations of motion are very similar except for a small depolarization after the end of motion for the longer duration trials (Fig. 4*B*, lower traces). During flight, however, we observed a quite large increase in baseline fluorescence and an increase of the response to visual motion with increasing stimulus duration (Fig. 4*B*, upper traces). For all durations, the GCaMP6f signal exhibited a fast initial rise followed by a slow increase throughout stimulus motion. This increase in GCaMP6f response for longer stimulus durations during flight in the T4 and T5 cells could explain the prolonged plateau potentials in postsynaptic HS cells, which are present during flight but absent during quiescence. These results indicate that at least some of the changes in HS cell physiology caused by flight are due to modulation of upstream circuits. The slow rise in the GCaMP6f signals in the T4 and T5 cells during flight might also be interpreted as evidence for weak integration. However, the rise in fluorescence with increasing stimulus duration in the T4 and T5 cells is much slower and smaller than that observed in the HS cell terminals using the same calcium indicator, especially for the short duration trials.

Discussion

The optomotor responses of flies have served as a useful model system to study the neural mechanisms that underlie motion vision. Performing a variety of open-loop behavioral experiments, we have shown here that this reflexive behavior resembles a leaky integrated version of the visual stimulus and, thus, would be consistent with the optomotor system implementing PI control. Open-loop paradigms are a standard technique in system identification because they make it possible to provide an arbitrary error signal as input while measuring the resulting controller output, without the latter influencing the former as it would in an intact closed-loop system (1). Open-loop approaches have been widely used for the study of fly optomotor behavior (2, 24, 28–31). Whereas the slow, integrator-like dynamics of the steering response are obvious in some prior studies (29–31), their implication with regard to integral feedback had not been noted. Integration of sensory signals can serve functions in control systems other than correcting for steady-state error. For example, in the oculomotor system of vertebrates, a velocity signal is integrated to construct an estimate of eye position (32, 33). However, given the leakiness of the integration and the temporal frequency dependence of optomotor response in flies, temporal integration would not likely result in a very precise estimate of angular position. The dynamics inherent in the behavioral responses to constant visual motion might be viewed as a low-pass filter, but that classification is not incompatible with our interpretation of a PI controller. Given the widespread application of PI controllers in engineering, we suggest that our experiments uncovered an integral component in the feedback control system, and that its role is to correct for steady-state error. For a flying animal, even a tiny amount of unidirectional retinal drift, if uncompensated, could lead to continuous rotation or sideslip. By having an integral term in the feedback system, even minute amounts of retinal slip would quickly ramp up and enforce a compensatory reaction.

To implement an integral term that can explain the dynamics of the optomotor response requires a process with a very slow time scale. Our results suggest that such a process is mediated by the calcium dynamics in the presynaptic terminals of HS cells. HS cells are thought to underlie steering responses to large-field horizontal motion (3–6). Previous studies have shown that LPTCs in flies exhibit slightly different response properties during flight or walking compared with quiescence (18–21). We find prolonged plateau potentials for high temporal frequencies during flight compared with quiescence, which are likely caused by increased input from presynaptic T4 and T5 cells during flight. However, these changes in membrane potential of HS cells are insufficient to explain the time course of the behavior. Instead we propose that because of the slow accumulation and clearance of presynaptic calcium, the transient membrane potential changes of the HS cells are transformed into a chemical signal that approximates the function of temporal integration. This integration seems to be stronger during flight compared with quiescence at the temporal frequency studied, which is likely a consequence of the increased plateau potentials. We thus speculate that one important function of the state-dependent changes in HS cell physiology could be the temporal integration of visual motion during flight. Further studies will be needed to demonstrate whether the dynamics of the observed HS cell responses cause the observed behavior.

Calcium dynamics have been implicated in intracellular computations including temporal integration (34). However, in contrast to our findings, calcium in these cases causes prolonged activity by influencing the firing rate of the same neuron through opening of calcium-dependent ion channels rather than transmitter release. In our model, we expect that the calcium signal reported by GCaMP6f is indicative of the time course of transmitter release from HS cell terminals and subsequent activation of downstream neurons that drive motor neurons of wing steering muscles. This hypothesis is testable in future studies by recording from descending interneurons postsynaptic to HS cells or by manipulating presynaptic calcium levels in HS cells and measuring the behavioral output. Such a process does not necessarily limit the bandwidth of the HS cell system, because the cells are thought to make electrical synapses with some of their downstream targets (7, 35) and possess chemical release sites in their terminals (36). Thus, we speculate that the electrically mediated outputs of HS cells might report the proportional component of rotatory visual motion, whereas the chemically mediated output reports the integral component.

Our experiments indicate that the optomotor integrator saturates at a level that generates a bilateral difference in wing stroke amplitude of at least 20°. Several studies using 3D high-speed videography have captured the free flight maneuvers of flying *Drosophila* (26, 37–40), and it is curious to note that flies accomplish quite rapid maneuvers by using changes in wing motion that are small compared with this value and those measured in prior experiments using open-loop stimuli in tethered flight (41, 42). Thus, the integrator may rarely wind up to a high level in free flight, because small changes in wing motion are sufficient to produce the required levels of compensatory torque (43). However, extensive changes in wing stroke amplitude could be required in free flight to compensate for the imbalance created if one of the wings would be even slightly damaged, a function in which PI feedback would likely play an essential role.

Materials and Methods

Flies. For whole-cell recordings, flies containing R27B03-Gal4 (44) and UAS-2xeGFP were floating over a wild-type Canton S background for at least 10 generations and were selected for fluorescence 1 d before the experiment. One- to 2-d-old female flies were used. For calcium imaging experiments, 4- to 7-d-old female flies heterozygous for w+;UAS-GCaMP6f;+ (27) and either w-;+;R27B03-Gal4 or w-;+;R42F06-Gal4 (10) were used. Pure behavioral experiments were performed on 1- to 3-d-old female wild-type CS flies.

Electrophysiology and Two-Photon Calcium Imaging. Whole-cell patch-clamp recordings were performed as described (20, 21) by using electrodes with a resistance of 7–9 MΩ. Bath temperature was held constant at 22 °C throughout the whole procedure. Two-photon calcium imaging was

performed as described (20, 45). For HS cell terminals, we imaged a 50.3 × 68.8 μm region at 17.3 frames per s. For T4 and T5 cell terminals, we imaged a 100.5 × 40.3 μm region at 18.3 frames per s.

Behavioral Measurements. Left and right wing stroke amplitudes in the physiology setup were acquired as described (21) by using a camera-based system at frame rates of 40–50 Hz.

Visual Stimuli and Data Analysis. Visual stimuli were presented by using a cylindrical LED arena with a 570-nm peak wavelength for electrophysiology and behavior and 470 nm for calcium imaging. The arena covered ∼200° horizontally and 60° vertically with a resolution of ∼2.25°. Large-field visual patterns consisted of a square-wave grating (a sine-wave grating for m-sequence experiments) with spatial wavelength of 36° and maximal contrast. Stimuli were presented in random order. For a given open-loop trial to be included in the analysis, the fly had to be flying continuously from 0.5 s before the onset of the stimulus until the end of stimulus presentation. Each fly contributed at least one trial to every stimulus condition of an experiment. Before and after open-loop stimulus presentation, the flies performed closed-loop stripe fixation, i.e., the velocity of a vertical bar depended on the behavioral response of the fly. All data analysis was performed in Matlab and Python.

The m-sequence experiments were largely performed as described (24). For neuronal recordings, a 10th-order m sequence was used; for pure behavioral recordings, a 15th-order m sequence. During each trial, the m sequence was presented four times at four different frequencies (35, 50, 65, and 80 Hz), respectively. Short periods of nonflight were removed from the traces. Impulse responses were obtained by convolving the m sequence with the respective signal and then dividing the result by the absolute number of motion steps. The transfer function was obtained by transforming the impulse responses into the frequency domain, dividing the behavioral by the neuronal data, removing high frequency components (above 30 Hz), and transforming the results back into the time domain.

For the calcium imaging data from HS cell terminals, the 15% brightest pixels in the mean image of all frames were classified as region of interest and the 15% dimmest pixels as background. For T4T5 cell imaging, we choose the region of interest manually and defined the background as the 10% dimmest pixels. For each frame, we computed fluorescence (Ft) by subtracting the mean of the background pixels from the mean of the region of interest pixels. For each fly, we computed the mean Ft before stimulus onset for each trial in which the fly did not fly (F0). Our metric for response is (Ft – F0)/F0, which we call $\Delta F/F$ for brevity.

Before convolving membrane potential changes with the kernel shown in Fig. 3*G*, we subtracted a baseline for the quiescence and flight condition from all traces, estimated as the mean of the last 2 s of the flicker trial, in which the pattern appeared and remained stationary for 3 s. Responses during the closed-loop period before open-loop stimulation were set to zero. Rise and decay time constants as well as response delay of the kernel were obtained by performing a least-square fit between the estimated and measured response for the shortest (0.1 s) duration trial.

ACKNOWLEDGMENTS. We thank Anne Sustar for the confocal image of the *R27B03-Gal4* line. This work was supported by the Raymond and Beverly Sackler Foundation (B.S.), the Paul G. Allen Family Foundation (M.H.D.), and Air Force Office of Scientific Research Grant FA9550-10-1-0368 (M.H.D).

1. Astrom KJ, Murray RM (2010) *Feedback Systems: An Introduction for Scientists and Engineers* (Princeton Univ Press, Princeton, NJ).
2. Götz KG (1968) Flight control in Drosophila by visual perception of motion. *Kybernetik* 4(6):199–208.
3. Geiger G, Nässel DR (1981) Visual orientation behaviour of flies after selective laser beam ablation of interneurons. *Nature* 293(5831):398–399.
4. Haikala V, Joesch M, Borst A, Mauss AS (2013) Optogenetic control of fly optomotor responses. *J Neurosci* 33(34):13927–13934.
5. Hausen K, Wehrhahn C (1983) Microsurgical lesion of horizontal cells changes optomotor yaw responses in the blowfly Calliphora erythrocephala. *Proc R Soc Lond B Biol Sci* 219(1215):211–216.
6. Heisenberg M, Wonneberger R, Wolf R (1978) Optomotor-Blindh31 - Drosophila mutant of lobula plate giant neurons. *J Comp Physiol* 124(4):287–296.
7. Schnell B, et al. (2010) Processing of horizontal optic flow in three visual interneurons of the Drosophila brain. *J Neurophysiol* 103(3):1646–1657.
8. Hausen K (1982) Motion sensitive interneurons in the optomotor system of the fly. 1. The Horizontal Cells - Structure and signals. *Biol Cybern* 45(2):143–156.
9. Maisak MS, et al. (2013) A directional tuning map of Drosophila elementary motion detectors. *Nature* 500(7461):212–216.
10. Schnell B, Raghu SV, Nern A, Borst A (2012) Columnar cells necessary for motion responses of wide-field visual interneurons in Drosophila. *J Comp Physiol A Neuroethol Sens Neural Behav Physiol* 198(5):389–395.
11. Takemura SY, et al. (2013) A visual motion detection circuit suggested by Drosophila connectomics. *Nature* 500(7461):175–181.
12. Borst A, Haag J, Reiff DF (2010) Fly motion vision. *Annu Rev Neurosci* 33:49–70.
13. Reichardt W (1961) in *Sensory Communication*, ed Rosenblith A (John Wiley & Sons, New York), pp 303–317.
14. Duistermars BJ, Chow DM, Condro M, Frye MA (2007) The spatial, temporal and contrast properties of expansion and rotation flight optomotor responses in Drosophila. *J Exp Biol* 210(Pt 18):3218–3227.
15. Duistermars BJ, Care RA, Frye MA (2012) Binocular interactions underlying the classic optomotor responses of flying flies. *Front Behav Neurosci* 6:6.
16. Fry SN, Rohrseitz N, Straw AD, Dickinson MH (2009) Visual control of flight speed in Drosophila melanogaster. *J Exp Biol* 212(Pt 8):1120–1130.
17. Tuthill JC, Chiappe ME, Reiser MB (2011) Neural correlates of illusory motion perception in Drosophila. *Proc Natl Acad Sci USA* 108(23):9685–9690.
18. Chiappe ME, Seelig JD, Reiser MB, Jayaraman V (2010) Walking modulates speed sensitivity in Drosophila motion vision. *Curr Biol* 20(16):1470–1475.
19. Jung SN, Borst A, Haag J (2011) Flight activity alters velocity tuning of fly motion-sensitive neurons. *J Neurosci* 31(25):9231–9237.
20. Suver MP, Mamiya A, Dickinson MH (2012) Octopamine neurons mediate flight-induced modulation of visual processing in Drosophila. *Curr Biol* 22(24):2294–2302.
21. Maimon G, Straw AD, Dickinson MH (2010) Active flight increases the gain of visual motion processing in Drosophila. *Nat Neurosci* 13(3):393–399.
22. Heisenberg M, Wolf R (1979) On the fine-structure of yaw torque in visual flight orientation of Drosophila melanogaster. *J Comp Physiol* 130(2):113–130.
23. Tammero LF, Dickinson MH (2002) Collision-avoidance and landing responses are mediated by separate pathways in the fruit fly, Drosophila melanogaster. *J Exp Biol* 205(Pt 18):2785–2798.
24. Theobald JC, Ringach DL, Frye MA (2010) Dynamics of optomotor responses in Drosophila to perturbations in optic flow. *J Exp Biol* 213(Pt 8):1366–1375.
25. Ringach D, Shapley R (2004) Reverse correlation in neurophysiology. *Cogn Sci* 28(2):147–166.
26. Fry SN, Sayaman R, Dickinson MH (2003) The aerodynamics of free-flight maneuvers in Drosophila. *Science* 300(5618):495–498.
27. Chen TW, et al. (2013) Ultrasensitive fluorescent proteins for imaging neuronal activity. *Nature* 499(7458):295–300.
28. Roth E, Reiser MB, Dickinson MH, Cowan NJ (2012) A task-level model for optomotor yaw regulation in Drosophila melanogaster: A frequency-domain system identification approach. *2012 IEEE 51st Annual Conference on Decision and Control (CDC)* (IEEE), pp 3721–3726.
29. Egelhaaf M (1987) Dynamic properties of 2 control-systems underlying visually guided turning in houseflies. *J Comp Physiol A Neuroethol Sens Neural Behav Physiol* 161(6):777–783.
30. Wolf R, Heisenberg M (1990) Visual control of straight flight in Drosophila melanogaster. *J Comp Physiol A Neuroethol Sens Neural Behav Physiol* 167(2):269–283.
31. Tammero LF, Frye MA, Dickinson MH (2004) Spatial organization of visuomotor reflexes in Drosophila. *J Exp Biol* 207(Pt 1):113–122.
32. Cohen B, Komatsuzaki A (1972) Eye movements induced by stimulation of the pontine reticular formation: Evidence for integration in oculomotor pathways. *Exp Neurol* 36(1):101–117.
33. Robinson DA (1989) Integrating with neurons. *Annu Rev Neurosci* 12:33–45.
34. Major G, Tank D (2004) Persistent neural activity: Prevalence and mechanisms. *Curr Opin Neurobiol* 14(6):675–684.
35. Haag J, Wertz A, Borst A (2010) Central gating of fly optomotor response. *Proc Natl Acad Sci USA* 107(46):20104–20109.
36. Raghu SV, Joesch M, Borst A, Reiff DF (2007) Synaptic organization of lobula plate tangential cells in Drosophila: γ-aminobutyric acid receptors and chemical release sites. *J Comp Neurol* 502(4):598–610.
37. Bergou AJ, Ristroph L, Guckenheimer J, Cohen I, Wang ZJ (2010) Fruit flies modulate passive wing pitching to generate in-flight turns. *Phys Rev Lett* 104(14):148101.
38. Fry SN, Sayaman R, Dickinson MH (2005) The aerodynamics of hovering flight in Drosophila. *J Exp Biol* 208(Pt 12):2303–2318.
39. Ristroph L, Berman GJ, Bergou AJ, Wang ZJ, Cohen I (2009) Automated hull reconstruction motion tracking (HRMT) applied to sideways maneuvers of free-flying insects. *J Exp Biol* 212(Pt 9):1324–1335.
40. Ristroph L, et al. (2010) Discovering the flight autostabilizer of fruit flies by inducing aerial stumbles. *Proc Natl Acad Sci USA* 107(11):4820–4824.
41. Götz KG, Hengstenberg B, Biesinger R (1979) Optomotor control of wing beat and body posture in Drosophila. *Biol Cybern* 35(2):101–112.
42. Lehmann FO, Dickinson MH (1997) The changes in power requirements and muscle efficiency during elevated force production in the fruit fly Drosophila melanogaster. *J Exp Biol* 200(Pt 7):1133–1143.
43. Dickson WB, Polidoro P, Tanner MM, Dickinson MH (2010) A linear systems analysis of the yaw dynamics of a dynamically scaled insect model. *J Exp Biol* 213(Pt 17):3047–3061.
44. Seelig JD, et al. (2010) Two-photon calcium imaging from head-fixed Drosophila during optomotor walking behavior. *Nat Methods* 7(7):535–540.
45. Weir PT, Schnell B, Dickinson MH (2014) Central complex neurons exhibit behaviorally gated responses to visual motion in Drosophila. *J Neurophysiol* 111(1):62–71.